

See discussions, stats, and author profiles for this publication at: <https://www.researchgate.net/publication/314272010>

A Bayesian Inference Tool for Geophysical Joint Inversions

Article · January 2016

DOI: 10.1071/ASEG2016ab131

CITATIONS

6

READS

158

5 authors, including:



[Graeme R Beardsmore](#)

Hot Dry Rocks Pty Ltd

47 PUBLICATIONS 476 CITATIONS

[SEE PROFILE](#)



[Simon O'Callaghan](#)

The Commonwealth Scientific and Industrial Research Organisation

24 PUBLICATIONS 275 CITATIONS

[SEE PROFILE](#)

Some of the authors of this publication are also working on these related projects:



Portable electronic divided bar [View project](#)



Geothermal Potential of Victoria [View project](#)

A Bayesian inference tool for geophysical joint inversions

Graeme BEARDSMORE*

Hot Dry Rocks Pty Ltd
PO Box 251
South Yarra
VIC 3141 AUSTRALIA
graeme.beardsmore@hotdryrocks.com

Hugh DURRANT-WHYTE

Centre for Translational Data Science
School of Information Technologies
University of Sydney, Darlington
NSW 2008 AUSTRALIA
hugh.durrantwhyte@sydney.edu.au

Lachlan McCALMAN

Data 61
Australian Technology Park
13 Garden Street, Eveleigh
NSW 2015 AUSTRALIA
lachlan.mccalman@data61.csiro.au

Simon O'CALLAGHAN

Data 61
Australian Technology Park
13 Garden Street, Eveleigh
NSW 2015 AUSTRALIA
simon.ocallaghan@data61.csiro.au

Alistair REID

Data 61
Australian Technology Park
13 Garden Street, Eveleigh
NSW 2015 AUSTRALIA
alistair.reid@data61.csiro.au

SUMMARY

Geophysical joint inversions seek to exploit the statistical fact that a model that simultaneously satisfies two or more independent data sets is more likely to represent geological 'reality' than a model that only satisfies a single data set. Interpreting geophysical data directly rapidly exceeds the capacity of a human as more data are added, so some form of machine assistance is usually required. Conventional inversion techniques can produce a 'best fit' model but this might only be one of a large range of possible models that fit the data. Bayesian inference provides a tool to evaluate the relative probability of *all* possible geological models in a given set, thereby quantifying the amount of information the data is actually providing.

Over 2012–2014, National ICT Australia (NICTA; now Data 61) worked with a number of university, government and industry partners, with support from the Australian Renewable Energy Agency, to build a Bayesian inference software tool for geophysical joint inversions. The tool was initially directed at geothermal energy exploration but is equally applicable to investigating other geological problems. For one geothermal exploration problem, Bayesian inference allowed us to jointly invert gravity, magnetics, magnetotelluric soundings and borehole temperature records to map in three dimensions the probability of encountering granite >270°C beneath the Moomba region of South Australia. The results correlated well with an independent deterministic inversion carried out by Geoscience Australia, but provided a much richer interpretation in probability space.

NICTA released the software tools as open source code on the GitHub platform.

Key words: Bayesian inference; Geophysical joint inversion; Cooper Basin; Moomba; Geothermal energy

INTRODUCTION

A basic tenet of geophysics is that any given geophysical sensor responds in a unique and predictable way to a given body of rock. For example, a gravity meter will always give the same measurement of gravitational acceleration at the same location (within measurement uncertainty, when all appropriate corrections are applied, and given no significant changes in subsurface density between measurements). Likewise, two-way-travel time will always be the same between given source and receiver locations for a seismic wavelet reflecting off a sub-surface horizon; electromagnetic soundings repeated in the same location will produce the same frequency or time spectra; and so on. This premise is based on established laws of physics and assumptions that the bulk physical properties of undisturbed rock formations (density, magnetic susceptibility, sonic velocity, thermal conductivity, electrical resistivity and so on) do not change rapidly on human timescales. Armed with physical laws and rock properties we can predict, or 'forward model', the unique geophysical 'signature' of any given combination and distribution of geological formations.

The reverse, however, is not true. Given a set of geophysical observations, we cannot unambiguously reconstruct the geological conditions that gave rise to the observations. In mathematical terms, the problem is 'under-determined'. That is, the number of geological variables that influence the geophysical observation is greater than the number of constraints provided by the observations. Gravity provides a simple example. The variation in gravitational acceleration across the Earth's surface is a function of the distribution of density within the Earth. But any finite set of gravity observations could be produced by an infinite variety of different density distributions. Some can be ruled out on practical grounds (for example, the density of a rock unit must be $> 0 \text{ g/cm}^3$), but there will always be an infinite set of density, depth and shape combinations that could produce the observations.

This is a fundamental problem for geophysicists because the ultimate goal of any geophysical observation is to understand the subsurface. What good is geophysics if it cannot provide a unique solution? Geophysicists address this problem by implicitly or explicitly incorporating prior knowledge and/or other data sets into any interpretation. Prior knowledge might include the expected general spatial relationships between rock units (for example, intrusive units cross-cutting older formations) or reasonable limits on possible rock properties. Other data might come from other geophysical tools, geological observations, or both. Information such as the depth to formation boundaries intersected by boreholes; the physical properties of representative rocks measured *in situ* or in a

laboratory; the general shape of formation boundaries imaged by seismic reflection; fault orientations and throws observed at the surface; and so on, all help to constrain the range of possible models.

A single model that simultaneously matches all known data provides a *more probable* representation of the true geology than a model that only satisfies a single data set. Put another way, the greater the number of independent data sets that a single model can satisfy, the greater the confidence we can have that the model accurately represents reality. This is the motivation for ‘joint inversion’ techniques; for example, simultaneously interpreting both gravity and magnetic data using a single model. We can have greater confidence in the joint solution than we can for a solution that only satisfies the gravity or magnetic data on their own.

Joint inversions also provide greater value than the ‘sum of their parts’ when the different data sets are sensitive to different aspects of the geology. For example, potential field techniques are most sensitive to lateral changes in geology, while seismic reflection and refraction techniques are more sensitive to vertical changes.

While most geophysicists recognise the power of joint inversion, however, putting it into practice can be exceedingly challenging for more than a very small number of data sets. Exploring the range of all possible models to find a simultaneous optimal fit to numerous data sets very quickly exceeds the limits of human capability.

Apart from the computational challenge of joint inversion, any inversion algorithm that produces a single solution introduces a risk that might not be immediately obvious. A single solution might converge on the *most probable*, representation of the true geology, but it is never the *only possible* solution. There may be other, very different, possible solutions with only marginally lower likelihood. Alternatively, the most probable solution could just be the median on a broad continuum of almost equally likely solutions. A far richer interpretation of the geophysical data is obtained from estimating the relative likelihoods of *all* possible points in the given model space. This is where a ‘Bayesian inference’ approach can be applied to geophysical inversion.

While computationally challenging, Bayesian inference is increasing being applied to geoscience problems. In the past few years, Bayesian inference has been used, for example, to make sense of mixing models of isotopic tracers in glaciers (Arendt et al., 2015); to reconstruct the relative plate motions of Nubia/Somalia before 3.2 Ma (Laffaldano et al., 2014); to investigate the crustal structure of southeast Australia from seismic noise topography (Young et al., 2013); to understand slip rates on the San Andreas Fault (Murray et al., 2014); to reconstruct sediment thermal histories in a probabilistic sense (Gallagher, 2012); to map the thickness of the Australian crust with uncertainties (Bodin et al., 2012); and to investigate the compositional and thermal structure of the lithosphere from geochemical evidence (Afonso et al., 2013). To the best of our knowledge, however, Bayesian inference has not yet been applied to joint geophysical inversion.

In March 2012, the Australian Centre for Renewable Energy awarded a grant to National ICT Australia (NICTA) to develop a methodology and software tools to apply Bayesian techniques to explore for geothermal energy. NICTA partnered with the University of Sydney, Australian National University, University of Adelaide, University of Melbourne, Geodynamics Ltd, Petrathem Ltd, Hot Rock Ltd, the Geological Survey of Victoria and the South Australian Department for Manufacturing, Innovation, Trade, Resources and Energy on what was ultimately a \$6.6 million, 27-month project. The outcome was a library of open source code for implementing a Bayesian inference approach to joint geophysical inversion. While developed for the specific purpose of geothermal exploration, the code is immediately relevant for many other geological targets. This paper presents the methodology developed for the project, using the geothermal case as an example and referring to the software as appropriate.

BAYESIAN INFERENCE

Bayes’ Theorem is a fundamental element of probability theory. It can be expressed as:

$$P(\theta|\mathbf{d}) = \frac{P(\theta)P(\mathbf{d}|\theta)}{\int P(\theta)P(\mathbf{d}|\theta)d\theta} \quad \text{Equation 1}$$

It is instructive to break Bayes’ Theorem into its individual terms to explain their meanings in a geophysics context. The paragraphs below introduce the different terms, while the following sections provide an example of the application of Bayesian geophysical inversion from NICTA’s geothermal energy project.

$P(\theta|\mathbf{d})$ can be read as “the probability that a particular geological model (θ) is ‘true’, given the observed set of data (\mathbf{d}).” In other words, how likely is it that the model we are investigating represents the ‘true’ geology given what we know in terms of geophysical (and other) data? This is a key question, for example, when we are faced with the financial risk of a drilling program. If we choose a drilling location and depth based on geophysical modelling, how likely is it that the drill will encounter the conditions, or discover the anomalous body, that our model predicts? Conventional inversion techniques usually search within a narrow range of possible models to find one that ‘best’ fits the data, but they don’t answer this question. Just because a model perfectly fits the available data does not necessarily mean it has $P(\theta|\mathbf{d}) = 1$; there might be other models that also perfectly fit the data. Bayes’ Theorem provides a rigorous means to quantify $P(\theta|\mathbf{d})$, but only if we can quantify the terms on the right hand side of Equation 1.

$P(\theta)$ can be read as “the *a priori* likelihood of a particular geological model (θ) occurring in nature.” This is the domain of the geologist. This value derives from reasonable geological constraints on what is, and is not, a possible geological model. The ‘prior’ is

constrained by such things as realistic ranges of rock property values; the law of geological superposition; expected maximum and minimum depths to principal geological boundaries; expected degree of curvature of formation boundaries; the likely ranges of dips, strikes, plunges and throws of layers, faults and folds; and so on (Figure 1).

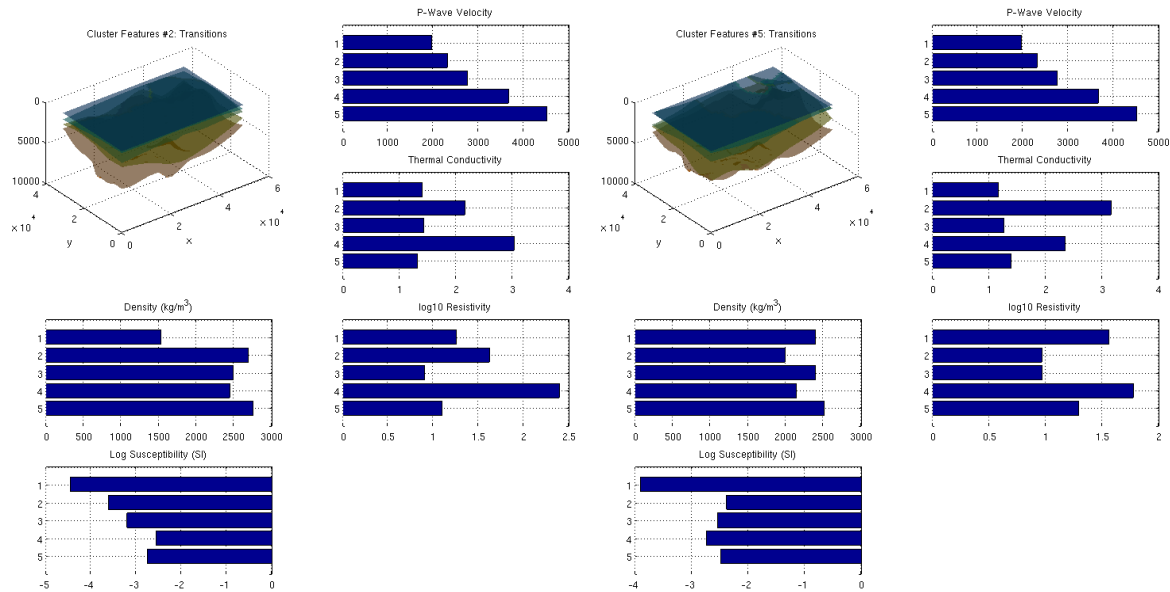


Figure 1: Two examples of geological models drawn from the same ‘prior’. The models are defined by five individual formations with rock properties drawn randomly from pre-defined probability distributions. The depths and shapes of formation boundaries are likewise defined by random selections from pre-constrained possibilities.

The *a priori* likelihood of any specific geological model is the statistical likelihood of the combination of parameters that define the model. Each individual parameter defining a geological prior could be expressed as a probability distribution. For example, a geologist might be very confident that the average density of Formation X lies between 2.20 g/cm³ and 2.50 g/cm³, with a most likely value of 2.35 g/cm³. In this case, the density of Formation X could be defined as a normal (or Gaussian) probability distribution with a mean of 2.35 g/cm³ and a standard deviation of 0.05 g/cm³ (three standard deviations covers 99.7% of all occurrences.) Not all parameters are independent. For example, the density and sonic velocity of rocks tend to be correlated in that a denser rock is likely to have higher velocity. Such a correlation can be incorporated into a prior so that random draws with high density and velocity are much more likely than draws with high density and low velocity.

$P(\mathbf{d}|\theta)$ can be read as “the probability that a particular geological model (θ) could produce the observed set of data (\mathbf{d}).” This is the domain of the geophysicist, and relies on forward modelling. For a specific geological model drawn from the prior, how well does the predicted geophysical response match the observed geophysical data (Figure 2)? In practice, this means constructing a numerical model of the geology defined by the parameters in the prior, using forward models to predict the geophysical response to the modelled geology, then comparing the prediction against the observed geophysical data. The ‘goodness of fit’ across all geophysical data sets must be distilled into a single ‘likelihood’ value between 0 and 1. There are challenges around how to treat measurement uncertainty and different quality data sets (e.g old data versus modern data), but there are also robust statistical rules and strategies for addressing these challenges. A single model and its likelihood define a single point within the ‘posterior’ of the Bayesian process. The full posterior covers all possible models and their likelihoods.

The denominator on the right hand side of Equation 1 is the integral of the numerator over all possible combinations of parameter values. This is the domain of the mathematician, computer scientist and statistician. In effect, a solution to Equation 1 requires that every possible geological scenario be tested against the observed geophysical data. While the range of possible models is constrained by the prior, there are still infinite combinations of randomly distributed parameters to consider within that range.

One approach is to attempt to sample from the distribution in Equation 1, rather than directly compute the integral. The resulting samples can be used to answer particular probabilistic queries about the inversion. The Markov-Chain Monte Carlo (MCMC) technique provides a tractable algorithm to perform this sampling, even on high-dimensional model spaces. However, when the forward models are computationally expensive, MCMC still requires the efficient allocation of computing resources.

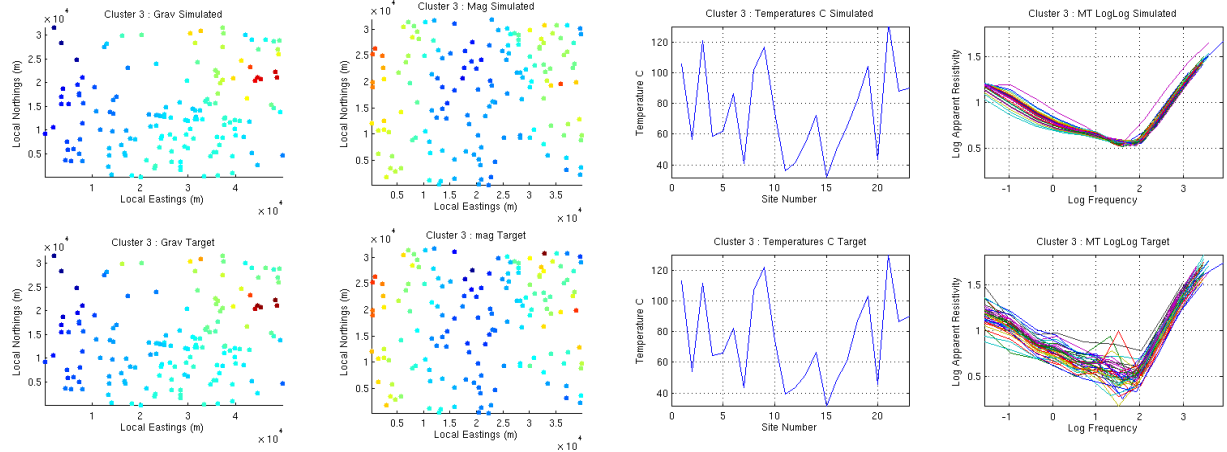


Figure 2: An example of a set of gravity, magnetic, borehole temperature and magneto-telluric responses (top row) forward modelled from a specific geological model, compared to the set of observed geophysical data over the same area (bottom row). $P(d|\theta)$ captures how closely these two sets match each other.

$P(\theta)$ — THE PRIOR

The power of Bayesian inference for geophysical inversion can be illustrated with a case study. One of the geological problems we investigated during our project was to infer the location of high temperature granitic rocks from geophysical and geological data sets. The specific aim was to infer the probability of high temperature granitic bodies in the basement in the vicinity of the Moomba gas field in NE South Australia. The first step in the Bayesian process was to ‘parameterise’ the geology. That is, for an area roughly 35 km x 35 km by 12 km deep we described the Cooper–Eromanga Basin and underlying basement as a finite set of parameters, each with mean and standard deviation values, encapsulating the range of possible geometries and physical properties of the rocks.

We divided the stratigraphy into six layers, based on natural groupings of physical properties such as thermal conductivity (Beardsmore, 2004; Figure 3), density and sonic velocity. The first layer extended from the surface to the top of Murta Formation. The Murta Formation underlies the Cadna-owie Formation, the top of which corresponds to a seismic reflection horizon interpreted and published by the Department of State Development (DSD) in South Australia (‘C-Horizon’; Figure 4). A scattering of well logs from the region indicated that the Cadna-owie formation has a relatively uniform thickness of about 70 m in the study area. We defined the top of the second layer, therefore, as 70 m below the depth-converted C-Horizon and added a degree of uncertainty to the depth as described below.

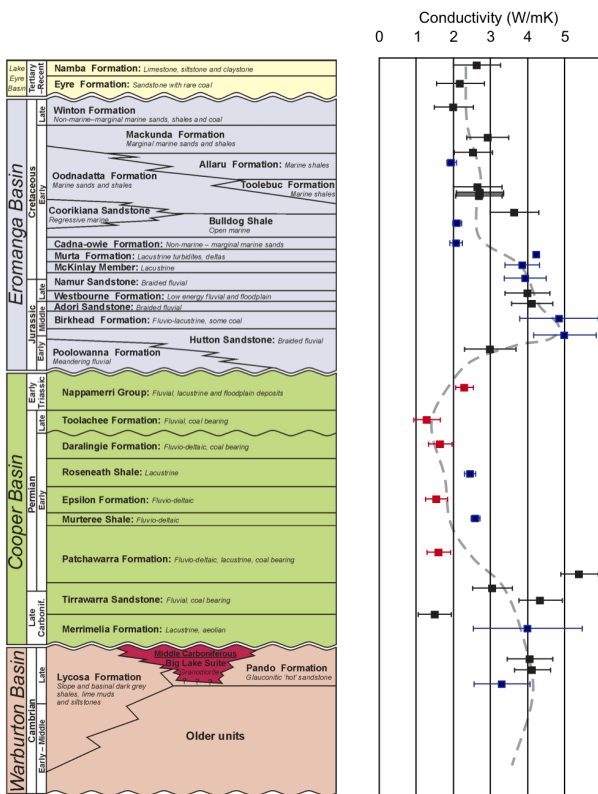


Figure 3: Thermal conductivity profile through the Cooper–Eromanga sequence. From Beardsmore (2004).

The top of the third layer corresponded to the top of the Namur Sandstone. The average interval between the tops of the Murta Formation and Namur Sandstone was 56 metres in boreholes around the region, with a standard deviation of less than 6 metres. So we defined the top of Layer 3 as 56 m below the top of Layer 2. The top of the fourth layer corresponded to the top of the Toolachee Formation, which we defined as 71 m above the depth-converted seismic ‘P-Horizon’ published by DSD, plus a degree of uncertainty. We divided the basement into two lithological groups. Layer 5 represented ‘granitic’ basement and Layer 6 ‘non-granitic’ basement. DSD’s depth-converted ‘Z-Horizon’ represents the top of the basement, but does not discriminate between Layer 5 and Layer 6. Furthermore, even where it has been intercepted by drilling, the vertical extent of Layer 5 (ie granitic rocks) is not known. We assumed that, where it exists, Layer 5 is of finite thickness and sits atop Layer 6 (ie non-granitic) rocks. Figure 5 summarises our six layers.

The mean depths and shapes of the interfaces between most layers were thus directly related to the depth-converted seismic horizons. To these surfaces we added uncertainty ranges with control points that could randomly deform each horizon in the vertical direction. The resulting surface was the sum of the horizon and a kernel-smoothed height-map of gridded points with parameterized heights.

Each layer was assigned a suite of rock properties relevant to the geophysical data sets we were inverting. The ranges of property

values were constrained by laboratory measurements on 115 core samples drawn from throughout the stratigraphic section. Properties of interest included density, magnetic susceptibility, thermal conductivity, radiogenic heat generation and electrical resistivity. Table 1 summarises the ranges of values we allowed our Bayesian model to explore. The properties of each layer were assumed to be constant across the entire layer. The prior distribution over rock properties was determined statistically from a combination of sample data and published averages.

Through the process described above, we could fully define (or parameterise) a geological framework for the Moomba study area, including the geometry of layer interfaces and physical rock properties, with a sequence of 101 numbers. Randomly drawing a value for each of the parameters from within their probability distribution effectively defined a single geological model conforming to our prior belief of what is possible. Each such random model had a unique combination of layer shapes, depths and physical properties.

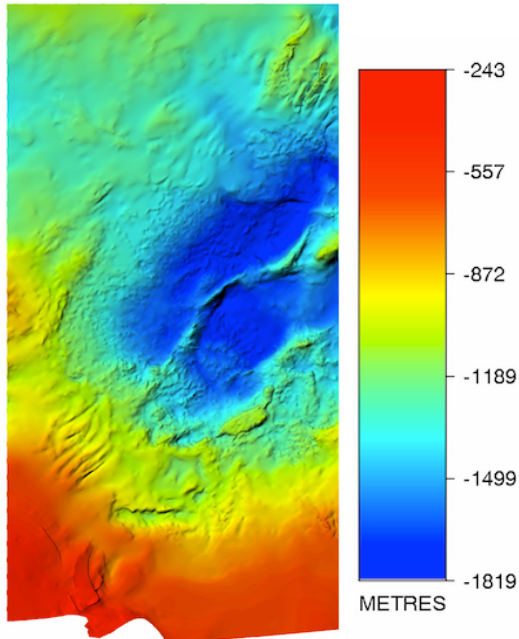


Figure 4: Depth to C-Horizon. Data supplied by the Department of State Development, South Australia.

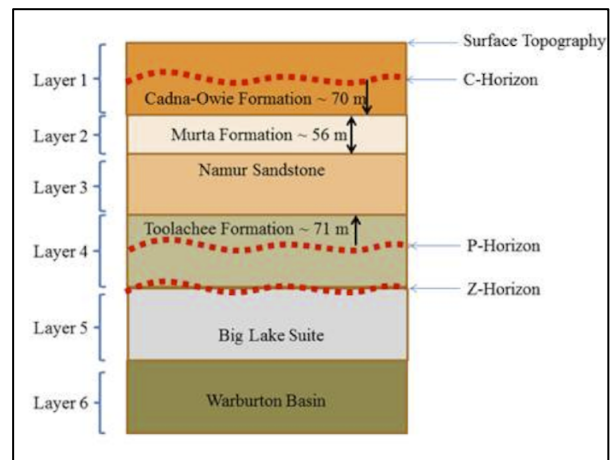


Figure 5: Summary of our stratigraphic layers.

Table 1: Mean values (standard deviation) of the a priori distributions of rock properties

Unit	Density (kg/m ³)	Magnetic Susc. (x10 ⁻⁵ SI)	Thermal Conductivity (W/mK)	Heat Production (μW/m ³)	Resistivity (Log ₁₀ Ohm.m)
Layer 1	2168 (239)	29.45 (7.09)	1.659 (0.20)	0.99 (0.71)	0.5 (0.2)
Layer 2	2572 (307)	78.03 (132.8)	2.15 (0.05)	1.83 (1.31)	0.9 (0.2)
Layer 3	2451 (131)	5.65 (12.64)	2.85 (0.05)	1.12 (0.89)	1.99 (0.73)
Layer 4	2390 (411)	2.49 (6.36)	1.35 (0.10)	1.56 (1.09)	2.17 (0.72)
Layer 5	2610 (42)	13 (3)	2.45 (0.05)	5 (1)	3.5 (0.5)
Layer 6	2680 (98)	47.23 (39.76)	2.40 (0.10)	1.74 (1.05)	1.56 (0.25)

$P(d|\theta)$ — FORWARD MODELS

For each random model drawn from our prior, we could forward model the expected responses of a range of geophysical sensors and compare the predictions against observed geophysical data. We had data in the form of Bouguer gravity values at a number of discrete locations; total magnetic field intensity at discrete locations; borehole temperature measurements at discrete depths and locations; and magnetotelluric soundings at discrete locations. For each of our random geological models, therefore, we solved for the expected surface gravitational acceleration; total magnetic field intensity (ignoring any potential remnant magnetism); temperature distribution assuming 3D steady state conductive heat flow; and 1D anisotropic apparent electrical resistivity versus frequency. Figure 6 shows an example set of forward model results compared against the observations.

Once the suite of geophysical predictions was generated, the next task was to statistically compare the predictions against the observations to determine a single ‘likelihood’ value for that particular geological model. The likelihood distributions were Gaussian

over the sensor measurements with mean equal to the simulated observation and unknown variance. We placed an inverse gamma prior on the unknown variances, and integrated analytically to produce a ‘Normal Inverse Gamma’ (NIG) likelihood.

In principle, there is no restriction on the number or type of forward models that we could include in the joint inversion. There are, however, some practical limitations. Firstly, each forward model must directly relate to an observed set of data. There is no value in forward modelling (for example) seismic wave speed anomalies if there are no seismic network data against which to compare the modelling results. Secondly, to achieve a practical Bayesian inference outcome for a high dimensional problem within a reasonable time frame, each forward model should be solvable in less than one second. This tends to rule out 4D models such as (for example) those involving fluid flow histories. Thirdly, there are always restrictions on available processing capacity and time that limit the ‘complexity’, or number of parameters that can be used to define the problem. Each additional data set included in the joint inversion requires additional parameters in the geological model to define the relevant rock properties.

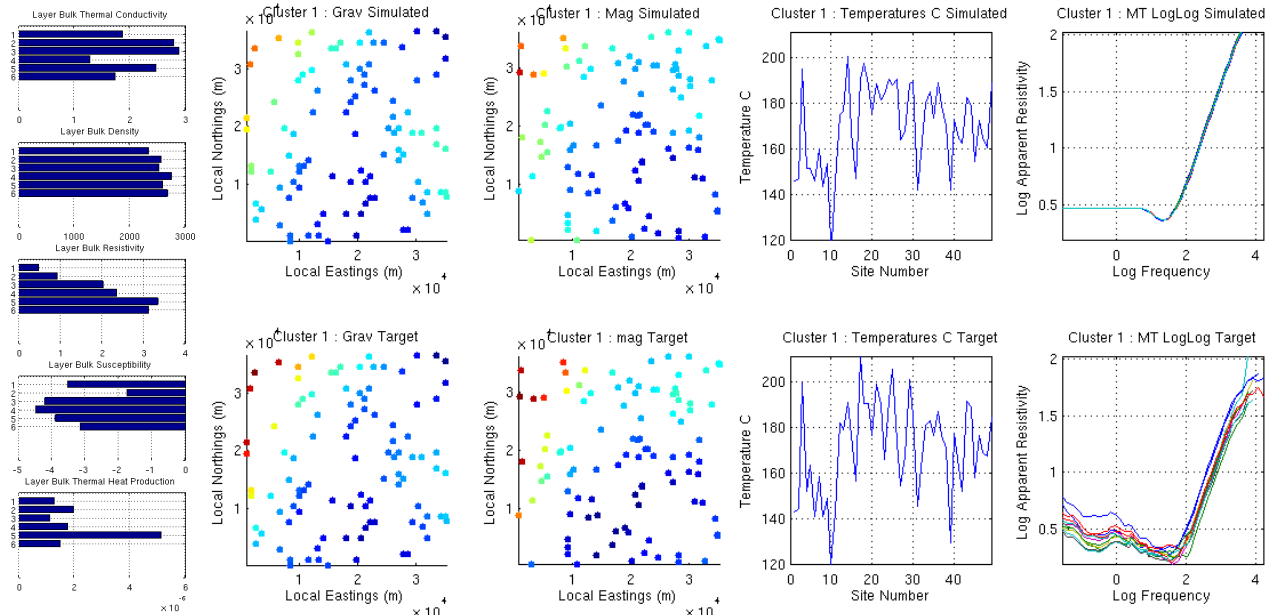


Figure 6: Left—Example random draw of rock properties, and; Right—Comparison between forward modelled predictions (top) and observations (bottom) for gravity, magnetics, ground temperature and apparent resistivity. (Note that the temperature charts are arbitrary representations of temperature at about 50 discrete points within the 3D model.)

EFFICIENT SAMPLING AND JOB ALLOCATION

The scope of this paper does not permit a detailed description of algorithms for sampling high dimensional spaces (such as the Moomba example with 101 variables described above). Suffice to say that sampling from the posterior of the Moomba model was complicated by the fact that the posterior was strongly underdetermined given the available geophysical observations. This means it is likely that there will exist distinct combinations of parameter values with high probability, separated by gulfs of low probability. Traditional MCMC sampling struggles to identify all probable combinations in this case, as a chain is very likely to get stuck in a local mode and be unable to step between probable regions. To combat this, we implemented an MCMC variant called ‘parallel tempering’, which uses multiple chains with different acceptance criteria that can exchange states under certain conditions. High ‘energy’ chains are weighted toward accepting new samples, exploring new parts of the parameter space, and can exchange with lower energy states when they discover regions of high probability. Ultimately, the algorithm provides us confidence that we have sampled across all disparate but probable regions of the posterior.

Another advantage of parallel tempering when one is interested in optimising computational efficiency is that likelihood computations for each chain can be computed in parallel. This allowed us to utilise cluster-computing resources to dramatically increase the number of samples computed in a given time. Additionally, because we assumed that the likelihood of each geophysical data set could be independently computed for each model drawn from the prior, we were also able to distribute the different sensor likelihood models to different cores.

Our implementation of the resulting algorithm, called ‘Obsidian’, takes advantage of cloud computing resources to distribute the joint inversion problem over approximately 40 nodes (160 cores) on Amazon Web Services (AWS). Obsidian is implemented in C++, and uses the ZeroMQ library to distribute computing jobs to worker nodes from a central server controlling the MCMC (Figure 7).

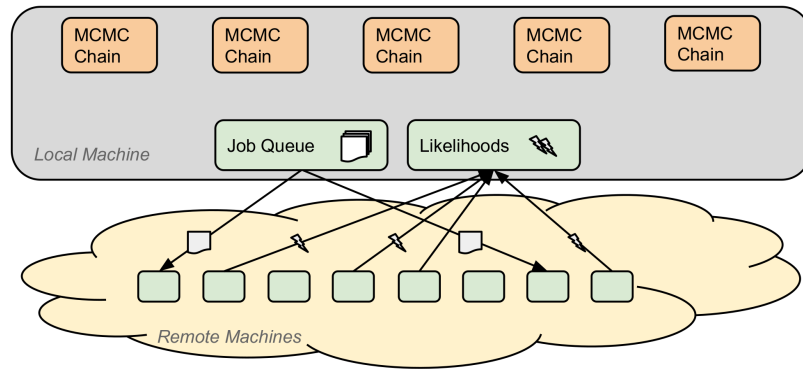


Figure 7: Schematic representation of how computing jobs are allocated between local and remote machines during an MCMC geophysical joint inversion.

$P(\theta|d)$ — OUTCOMES OR ‘POSTERIOR’

The outcome, or ‘posterior’, of Bayes’ Theorem in the context of geophysical joint inversion is a probability distribution of geological models based on how well they predict the available data. In situations with sparse data, the posterior might reveal many disparate families of models with similar probabilities of producing the observed data. In situations with lots of constraining data, however, the posterior might confirm that a certain family of models has a demonstrably higher probability of being ‘true’. What we are really interested in, however, is what the posterior can tell us about the particular problem in which we are interested. In the geothermal context, for example, we might want to know such things as, “What is the expected temperature at a given point in my region of interest?”, or “What is the probability that granite exists at any given point within my region of interest?”

Interrogating the model posterior with questions such as these implicitly involves considering all the possible combinations of parameters in the model. We can answer questions of this type by ‘marginalising’ over the set of samples obtained from MCMC. Marginalised distributions correspond to weighted averages of the property of interest given the parameters of each sample. Because the samples from the MCMC algorithm statistically represent the posterior distribution, the probability of having drawn a sample is proportional to its probability density in the distribution. In this case we can equally weight the samples. The answer to the first question can be found, therefore, from the mean of the distribution of temperatures across all the MCMC samples. Considerable additional value is gained by quantifying the uncertainty in terms of the standard deviation in the distribution (Figure 8). We can immediately see where the data provide maximum confidence in the expected temperature (blue regions of the right hand image in Figure 8) and where we lack sufficient information for a confident temperature prediction (orange to red regions).

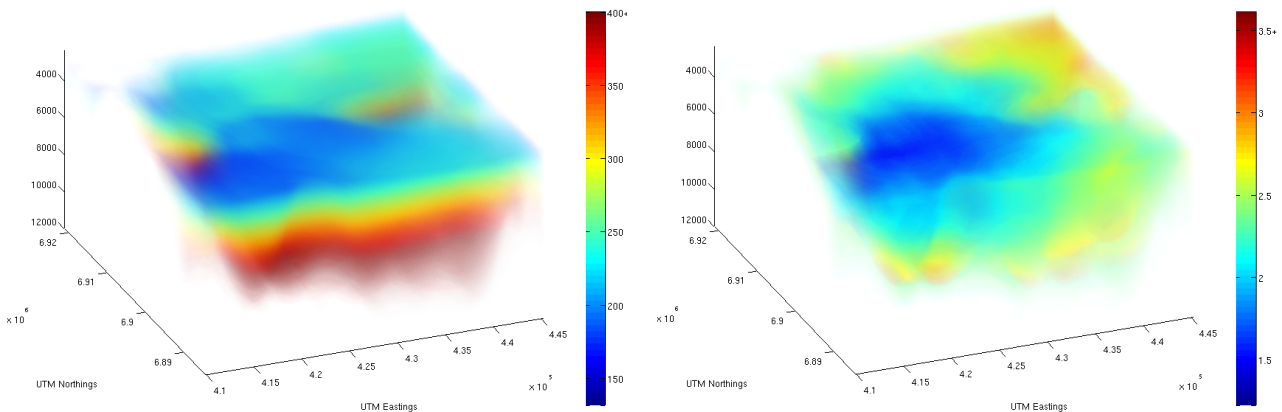


Figure 8: Left—The mean, or expected, temperature (°C) at each point in the Moomba model space. Right—The standard deviation (°C) in the expected temperature.

Regarding the second question above, the actual answer is a scalar value and does not express any of the specific parameters defining the model. For example, if 60% of our MCMC posterior sample includes granite at a particular depth and location, then the probability of granite being there is 0.6 (given the data and our prior distributions). Figure 9 illustrates this example by showing the probability that granitic basement occurs at any given point within our model space, given the data we had available at the time and the constraints we placed on our prior.

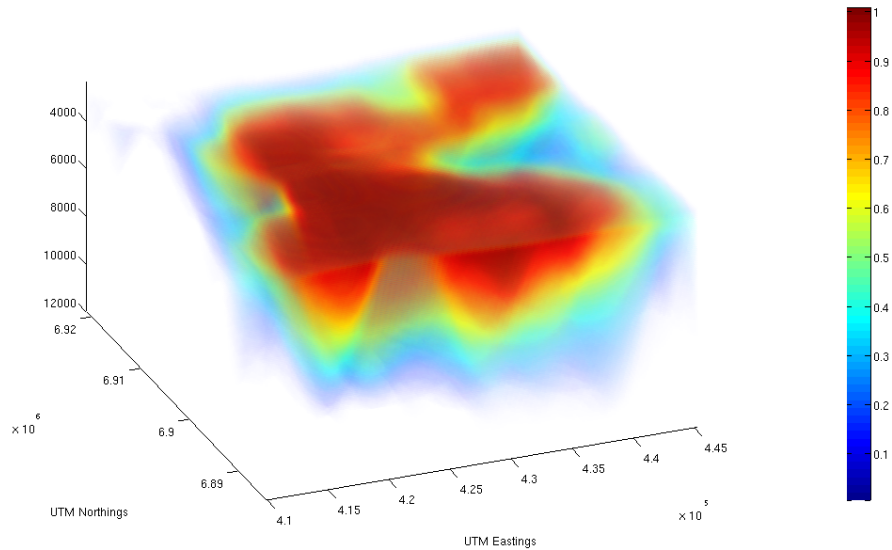


Figure 9: The probability that granitic basement exists at any given point within our model space. Red = granitic basement probably does exist; blue = granitic basement probably does *not* exist; green = existing data are insufficient to discriminate between granitic and non-granitic basement. Note that probability is represented by both colour and transparency.

Additionally, we can apply ‘non-trivial simulations’ on each sample, and the distributions of the derived property will be representative. This allows us to answer a broader set of questions such as, “What is the probability that granite exceeding 270°C exists at any given point within my region of interest?” The marginalisation propagates the uncertainty from the parameter space samples. Results can be visualised in the same way as above (e.g. Figure 10).

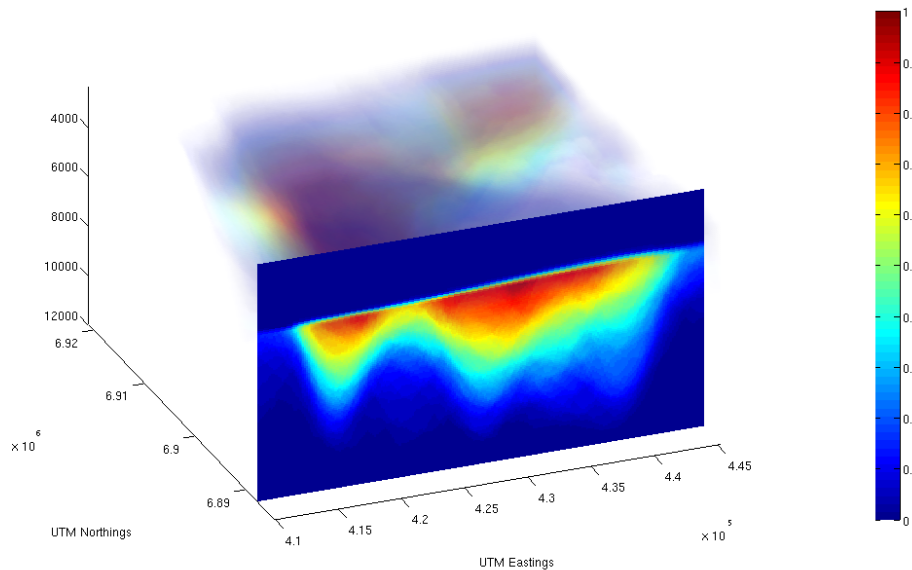


Figure 10: The probability that granitic basement exists *and* exceeds 270°C at any given point within our model space. The cross section is included to show detail.

While the images in Figures 8, 9 and 10 look vastly different to the outcomes of conventional geophysical inversions that many geoscientists would be familiar with (ie visual approximations of ‘real’ geological architectures), they arguably provide more useful information upon which to base investment decisions. If the primary goal of a company is to drill into granitic basement to intersect temperatures >270°C, then a well could be confidently planned to intercept the dark red zone on Figure 10. Furthermore, if the company preferred for some reason (e.g. limited extent of licence boundaries) to drill into a zone shown as green or yellow, it might choose to first carry out additional surface surveys to increase its confidence that the well would hit the desired target.

Figure 11 provides one last example to highlight the additional value that Bayesian inference can provide over conventional inversion techniques. It directly compares two predictions of the location of granitic basement beneath the Moomba region. The left hand map shows the deterministic outcome of a conventional gravity inversion by Geoscience Australia. It shows regions with predicted granitic basement (red) and regions without (white). The right hand map shows a probabilistic prediction for the same region based

on Bayesian joint inversion of gravity, magnetics, MT and temperature data, where red areas are ‘high probability’ and blue areas are ‘low probability’.

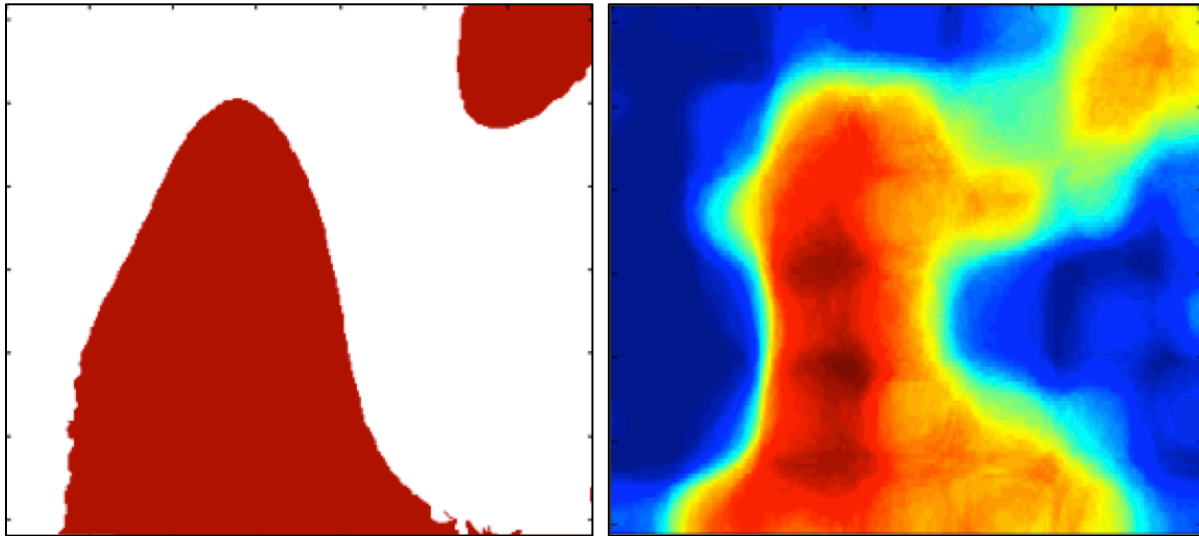


Figure 11: Two predictions of the location of sub-cropping granitic basement at 3500 m beneath the Moomba region. Left—Deterministic prediction by Geoscience Australia based on conventional 3D inversion of gravity data “using geological data to constrain the inversions” (Meixner and Holdgate, 2009). Right—‘Probability of granitic basement’ prediction by NICTA using Bayesian joint inversion of gravity, magnetics, MT and temperature.

While there is an obvious strong correlation between the two maps, the right hand map contains far more information about the confidence of the predictions. Of particular interest is the area in the northeast quadrant of the maps where Geoscience Australia predicts ‘no granite’ between two granitic sub-crops. The right hand map charts this area in green, indicating that there is, in fact, insufficient information to determine whether there is granite sub-crop or not.

CONCLUSIONS

A Bayesian approach to joint geophysical inversion can reveal the full probabilistic range of geological models that satisfy existing data. The Bayesian framework, in principle, allows joint inversion of any number of independent data sets. The results can be interrogated to provide a much deeper and richer understanding of the true state of knowledge compared to conventional inversion methods. Future exploration activities can be confidently planned around reducing uncertainties in key parameters or discriminating between different families of likely geological models. Current computing resources coupled with efficient sampling algorithms can provide solutions for geological models with up to 1000 degrees of freedom within reasonable timeframes. That number will grow as computing resources continue to increase in power and efficiency. The challenges around implementing Bayesian inference joint inversion relate to making the tools known, available and usable to a wide user base.

The ‘Obsidian’ software is open source and can be downloaded from <https://github.com/NICTA/obsidian>.

ACKNOWLEDGMENTS

The work reported in this paper was made possible by a grant from the Australian Renewable Energy Agency under contract No. 2410: “Data Fusion and Machine Learning for Geothermal Target Exploration and Characterisation.” Many individuals aside from the authors worked on that project. Technical project participants included (in no particular order) Darren Shen, Simon Carter, Lars Krieger, Edwin Bonilla, Fabio Ramos, Michelle Salmon, Malcolm Sambridge, Olena Velychko and Tim Rawling. More recently, David Cole has been involved in further refinement of the ‘Obsidian’ and related codes.

REFERENCES

- Afonso, J.C., Fullea J., Yang, Y., Connolly, J.A.D. and Jones, A.G., 2013, 3D multi-observable probabilistic inversion for the compositional and thermal structure of the lithosphere and upper mantle II: General methodology and resolution analysis: *Journal of Geophysical Research*, DOI:10.1002/jgrb.50123.
- Arendt, C.A., Aciego, S.M. and Hetland, E.A., 2015, An open source Bayesian Monte Carlo isotope mixing model with applications in Earth surface processes: *Geochemistry Geophysics Geosystems*, 16, 1274–1292. DOI:10.1002/2014GC005683.
- Beardsmore, G., 2004, The influence of basement on surface heat flow in the Cooper Basin: *Exploration Geophysics*, 35, 223–235.

- Bodin, T., Salmon, M., Kennett, B.L.N. and Sambridge, M., 2012, Probabilistic surface reconstruction from multiple data sets: An example for the Australian Moho: *Journal of Geophysical Research*, 117, B10307. DOI:10.1029/2012JB009547.
- Gallagher, K., 2012, Transdimensional inverse thermal history modeling for quantitative thermochronology: *Journal of Geophysical Research*, 117, B02408. DOI:10.1029/2011JB008825.
- Iaffaldano, G., Hawkins, R. and Sambridge, M., 2014, Bayesian noise-reduction in Arabia/Somalia and Nubia/Arabia finite rotations since ~20 Ma: Implications for Nubia/Somalia relative motion: *Geochemistry Geophysics Geosystems*, 15, 845–854. DOI:10.1002/2013GC005089.
- Meixner, T. and Holgate, F., 2009, The Cooper Basin Region 3D Geological Map Version 1: A search for hot buried granites: *Geoscience Australia, Record 2009/15*. 14pp.
- Murray, J.R., Minson, S.E. and Svarc, J.L., 2014, Slip rates and spatially variable creep on faults of the northern San Andreas system inferred through Bayesian inversion of Global Positioning System data: *Journal of Geophysical Research, Solid Earth*, 119, 6023–6047. DOI:10.1002/2014JB010966.
- Young, M.K., Cayley, R.A., McLean, M.A., Rawlinson, N., Arroucau, P. and Salmon, M., 2013, Crustal structure of the east Gondwana margin in southeast Australia revealed by transdimensional ambient seismic noise tomography: *Geophysical Research Letters*, 40, 4266–4271. DOI:10.1002/grl.50878.